FEBS 28816 FEBS Letters 576 (2004) 245–250

The *C. elegans* methionine aminopeptidase 2 analog *map-2* is required for germ cell proliferation

Mike Boxem[a,1], Chiawei W. Tsai[b,2], Yi Zhang[b,3], R. Mako Saito[a], Jun O. Liu[b,*]

[a] *Massachusetts General Hospital Cancer Center, Charlestown, MA 02129, USA*
[b] *Department of Pharmacology and Molecular Sciences and Department of Neuroscience, Johns Hopkins School of Medicine, East Baltimore Campus, Room 516, Hunterian Bldg., 725 North Wolfe St., Baltimore, MD 21205-2105, USA*

Received 6 June 2004; revised 12 August 2004; accepted 20 August 2004

Available online 18 September 2004

Edited by Ned Mantei

Abstract We have investigated the physiological function of type 2 methionine aminopeptidases (MetAP2) using *Caenorhabditis elegans* as a model system. A homolog of human MetAP2 was found in the *C. elegans* genome, which we termed MAP-2. MAP-2 protein displayed methionine aminopeptidase activity and was sensitive to inhibition by fumagillin. Down-regulation of *map-2* expression by RNAi led to sterility, resulting from a defect in germ cell proliferation. These observations suggest that MAP-2 is essential for germ cell development in *C. elegans* and that this ubiquitous enzyme may play important roles in a tissue specific manner.

Keywords: *map-1*; *map-2*; Methionine aminopeptidase; Germline development

1. Introduction

Processing of N-terminal methionines is an essential post-translational process in both prokaryotes and eukaryotes. This process is catalyzed by a highly conserved family of enzymes known as methionine aminopeptidases (MetAPs) [1,2]. In prokaryotes such as *Escherichia coli* and *Salmonella typhimurium*, a single methionine aminopeptidase gene has been identified, the deletion of which is lethal [3,4]. In eukaryotes, multiple genes have been found to encode this enzyme family. In both yeast and humans, two proteins are known to possess methionine aminopeptidase activity, which are known as type 1 (MetAP1) or type 2 (MetAP2) enzymes, respectively [5–7]. In addition, a third isoform that appears to be specific for the mitochondria has recently been discovered in mammals [8]. In yeast, knockout of either *MAP1* or *MAP2* causes a decrease in growth rate while elimination of both genes is lethal [6], indicating that the two MetAPs play redundant functions and are together essential for yeast proliferation.

Recently, we and others identified mammalian MetAP2 as a target for the angiogenesis inhibitors fumagillin and ovalicin [9–16], suggesting a role for MetAP2 in angiogenesis. The inhibition of angiogenesis by these natural products is due to inhibition of endothelial cell proliferation. Fumagillin and ovalicin show a surprising degree of selectivity; of a large number of primary human cells tested, endothelial cells are among the most sensitive to inhibition by fumagillin [17,18]. Thus, although methionine aminopeptidases appear to be universally important enzymes in prokaryotes and yeast, MetAP2 may play a more tissue and cell type specific role in higher eukaryotes.

Despite the apparent importance of MetAP2 in angiogenesis, little is known about the function of MetAP2 proteins in vivo. To better understand the physiological function of type 2 MetAPs in a multicellular organism, we turned to the *C. elegans* for the ease with which genetic manipulations can be carried out in the worm. We found a single predicted ORF (Y116A8A.9) with a high degree of similarity to human MetAP2 in the genome of *C. elegans*, which we termed *map-2*. We cloned the predicted *C. elegans map-2* gene, and overexpressed and purified MAP-2 protein from baculovirus-driven insect cells. We show that MAP-2 is a fully active methionine aminopeptidase and is sensitive to inhibition by fumagillin. We used RNA interference (RNAi) to inhibit the expression of *map-2* and observed defects in gonad development. Further analysis of this defect suggests a critical role for *map-2* in germ cell proliferation in *C. elegans*.

2. Materials and methods

2.1. Strains and culture conditions

Worm strains used were derived from the wild-type Bristol strain N2 and were cultured using standard techniques as described [19]. In addition to N2, the following strains and mutations were used: DG1576 *tnIs5[lim-7::GFP; rol-6(su1006d)]* [20] and NL2098 *rrf-1(pk1417) I* [21].

2.2. Purification of recombinant MAP-2 protein

The full-length *map-2* gene was PCR amplified from the ProQuest *C. elegans* cDNA library (Invitrogen) using primers 5′-GCGAATTC-ATGCCACCAGCAAACGGAAAAAAG-3′ and 5′-GCCTCGAG-TTAATAATCATCTCCACGGGAG-3′, then cloned into the

* Corresponding author. Fax: +1-410-955-4620.
E-mail address: joliu@jhu.edu (J.O. Liu).

[1] Present address: Department of Cancer Biology, Dana Farber Cancer Institute, Boston, MA 02115, USA.
[2] Present address: Malaria Vaccine Development Unit, National Institute of Allergy and Infectious Disease, National Institutes of Health, Rockville, MD 20852, USA.
[3] Present address: Memorial Sloan-Kettering Cancer Center, Box 576, 1275 York Avenue, New York, NY 10021, USA.

Abbreviations: MetAP, methionine aminopeptidase; MAP, methionine aminopeptidase; P.I., propidium iodide; ORF, open reading frame; RNAi, RNA interference; dsRNA, double-stranded RNA

0014-5793/$22.00
doi:10.1016/j.febslet.2004.08.077

pFastBacHT vector (Invitrogen). The resultant pFastbac-ceMAP2 construct was transfected into packaging cell line Sf9 (Pharmingen). Recombinant P2 baculovirus carrying *map-2* with a 6xHis tag was used to infect Hi5 insect cells. Sf9 and Hi5 monolayer cells were maintained in Grace's medium (Gibco). His-tagged MAP-2 was purified from Hi5 cells using a Talon metal affinity column (Clontech) and used for further enzymatic assays or stored at −80 °C.

2.3. RNAi

Gateway recombinational cloning (Invitrogen) was used to generate RNAi template constructs. For full-length *map-2* and F53B6.5, entry clones were obtained from the Vidal lab ORFeome resource [22]. For *map-2* 5′ and 3′ regions, entry clones were generated from fragments PCR amplified from the ProQuest *C. elegans* cDNA library (Invitrogen) with the following primers: for *map-2* 5′ region: 5′-GGGGACAAGTTTGTACAAAAAAGCAGGCTTGCCACCAGCAAACGGAA-3′ and 5′-GGGGACCACTTTGTACAAGAAAGCTGGGTTTCACGGACTGCTT CGAC-3′, and for *map-2* 3′ region: 5′-GGGGACAAGTTTGTACAAAAAAGCAGGCTACCAATGCCGGAATCAAAGAA-3′ and 5′-GGGGACCACTTTGTACAAGAAAGCTGGGTAATAATCATCTCCACGGGAGAC-3′. The inserts in each entry clone were transferred into the pDEST-pPD129.36 vector, which contains juxtaposed T7 promoter sites flanking the insert site [23]. From these constructs, linear template DNA was generated by PCR using primers 5′-TGGATAACCGTATTACCGCC-3′ and 5′-GTTTTCCCAGTCACGACGTT-3′. Double stranded RNA was then generated using the MEGAscript in vitro transcription kit (Ambion, Austin, TX). Animals were injected following standard procedure [19] and progeny produced more than 24 h after injection of dsRNA were examined.

2.4. DNA staining

DNA was stained with propidium iodide as previously described [24].

2.5. Ovalicin feeding

Between 1 and 10 L4 age N2 animals were placed in S-medium [19] with *E. coli* OP50 in 96-well plates. Different amounts of ovalicin (1:10–1:1 000 000 serial dilutions from a 10 mM stock) were added to each well. As ovalicin is unstable at lower pH levels, the pH of the S-medium was increased to 7. After growth at 20 °C for 3–5 days, the F1 generation was examined for phenotypic abnormalities.

2.6. Ovalicin injection

Young adult N2 animals were injected with 100 and 1000 μM final concentrations of ovalicin in M9 buffer [19], and their progeny was examined for phenotypic abnormalities.

2.7. Western blotting

To obtain *C. elegans* protein samples, wild-type and *map-2(RNAi)* animals were lysed by boiling in 1× Laemmli sample buffer [25]. Protein samples were subjected to SDS–PAGE and immunoblotted using standard techniques [25]. Antibodies used were polyclonal anti-human MetAP2, that was shown to react with the worm MetAP2 at 1:1000 dilution, and anti-Tubulin ab3194 (Abcam) at 1:1000 dilution.

3. Results

3.1. Identification of MetAP1 and MetAP2 orthologs in the genome of C. elegans

BLAST searches of the *C. elegans* genome identified one predicted ORF similar to yeast and human MetAP1 (Y37E11AL.7), and four predicted ORFs similar to yeast and human MetAP2 (Y116A8a.9, F53B6.5, T27A8.3 and W08E12.7) (Fig. 1A). Several lines of evidence indicate that these ORFs are predicted correctly. First, we were able to PCR amplify fragments of the expected size from a cDNA library using primers directed against the predicted 5′ and 3′ ends of the genes (not shown). Second, cDNAs exist that correspond to the predicted structures of Y37E11AL.7, Y116A8a.9 and W08E12.7 (http://www.wormbase.org, release WS123). Finally, the sequences between the putative start and stop of F53B6.5 and W08E12.7 have been verified by the ORFeome project [22].

Based upon sequence similarity, Y116A8a.9 is a strong candidate to be a functional MetAP2 enzyme. Of the four MetAP2 related ORFs, only Y116A8a.9 has high overall similarity to mammalian MetAP2 (Fig. 1A), is predicted to

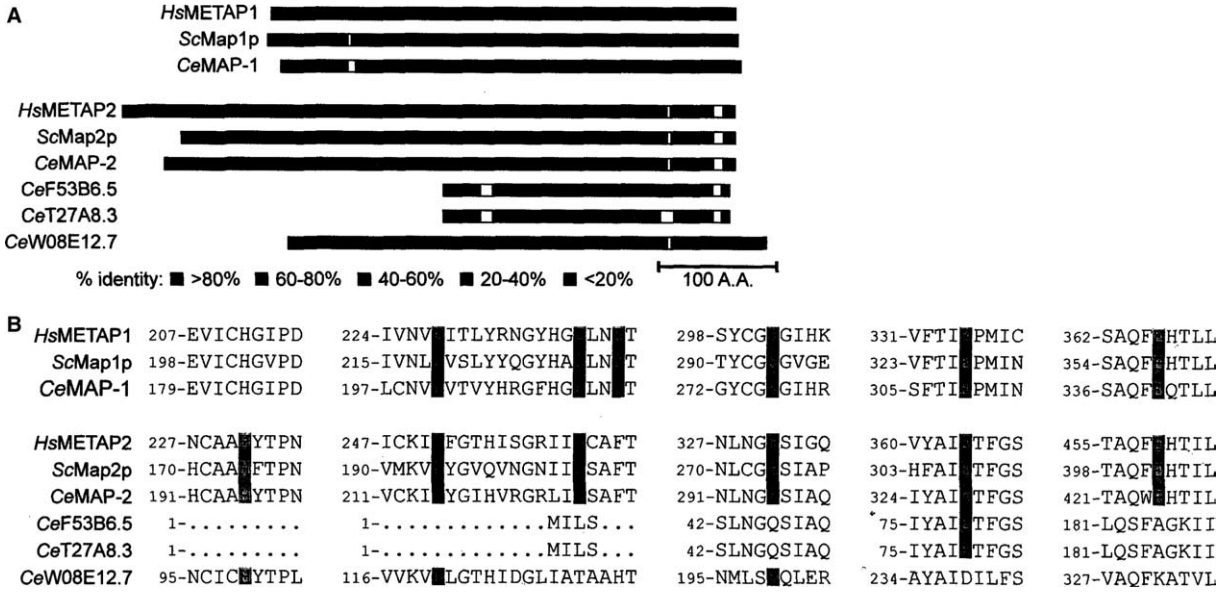

Fig. 1. Identification of *C. elegans* homologs of type I and II methionine aminopeptidases. (A) Sequence comparison between the human and *S. cerevisiae* MetAP proteins and their closest homologs in *C. elegans*. Proteins were aligned using the ClustalW algorithm and colored according to their amino acid identity with the human METAP proteins. (B) Conservation of residues in the active site involved in the binding of two metal ions. The numbers indicate the amino acid position within each protein sequence. Green box: the histidine covalently modified by fumagillin. Red boxes: metal-binding residues critical for aminopeptidase activity. In both panels, CeMAP-1 and CeMAP-2 refer to the predicted ORFs Y37E11AL.7 and Y116A8a.9, respectively.

encode the unique N-terminal extension characteristic of eukaryotic MetAPs (Fig. 1A), and contains all five critical residues in the active site of human and yeast MetAP2 proteins involved in the binding of two metal ions (Fig. 1B). Therefore, based upon the high degree of similarity between MetAP1 and Y37E11AL.7, and between MetAP2 and Y116A8a.9, we named the corresponding genes *map-1* and *map-2*, respectively (for methionine aminopeptidase), and selected Y116A8a.9 as the likely worm MetAP2 analog for further analysis.

3.2. *MAP-2 is an active methionine aminopeptidase and is capable of binding to fumagillin irreversibly*

To characterize MAP-2 biochemically, we overexpressed His-tagged MAP-2 in baculovirus-driven insect cells and purified the recombinant protein to near homogeneity with the help of the Talon metal affinity resin. Recombinant MAP-2 is active as a methionine aminopeptidase, as demonstrated by its ability to cleave a methionine-containing oligopeptide substrate, Met–Ala–Ala–Met (Fig. 2A) [12,26]. MAP-2 is similar in activity to human MetAP2, as judged by the amount of substrate cleaved at identical concentrations of these proteins (data not shown). We next determined whether MAP-2 is sensitive to fumagillin. As shown in Fig. 2A, the clinically tested fumagillin analog, TNP-470, inhibited MAP-2 activity in a dose-dependent manner. Using 10 nM of recombinant MAP-2, the IC_{50} value for TNP-470 was determined to be 310 nM. In comparison, the human enzyme has an IC_{50} value of about 10 nM under the same assay conditions. Thus, MAP-2 is significantly less sensitive to TNP-470. Although all key residues known to be involved in direct contact with fumagillin based on the crystal structure [11] are conserved between MAP-2 and human MetAP2, sequence divergence exists for residues in close proximity to those residues. Examples of sequence divergence include Asp178, Ala298, and Val416 in MAP-2 in place of Asn214, Gly334 and Ile450 in hMetAP2, respectively. These differences in sequence may account for the difference in sensitivity to TNP-470 between MAP-2 and human MetAP2 proteins.

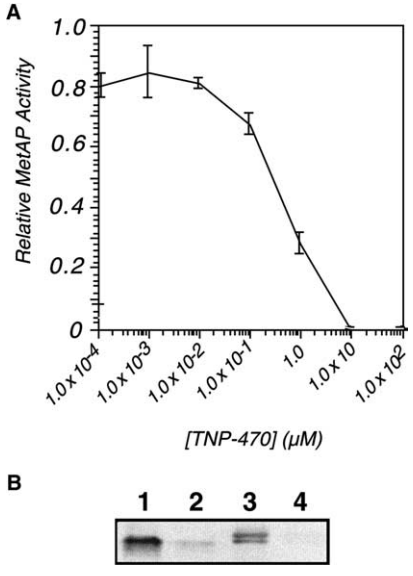

Fig. 2. MAP-2 is a functional methionine aminopeptidase and is inhibited irreversibly by fumagillin. (A) Inhibition of worm MAP-2 by TNP-470. Varying concentrations of TNP-470 were incubated with 10 nM of MAP-2 for 1 h before the enzyme activity was determined. The relative activity was obtained by normalizing enzyme activity to that determined in the absence of TNP-470. (B) MAP-2 binds to fumagillin irreversibly. Near-Western blot was performed using recombinant worm MAP-2 (Lanes 1 and 2) and human MetAP2 (Lanes 3 and 4). Lane 1, MAP-2 + Biotin-fumagillin; Lane 2, MAP-2 + Biotin-fumagillin + TNP-470; Lane 3, hMetAP2 + Biotin-fumagillin; Lane 4, hMetAP2 + Biotin-fumagillin + TNP-470.

Fumagillin was previously shown to bind to human and yeast MetAP2 by forming a covalent bond between the drug and protein through the opening of the spiro-epoxide of fumagillin by a histidine residue in the active site of MetAP2 [10–12]. As this histidine is conserved in MAP-2, we determined whether fumagillin is bound covalently to MAP-2 using the "Near Western" blot analysis developed previously [16]. Upon incubation of MAP-2 or human MetAP2 with a biotin-fumagillin conjugate, the reaction mixture was subjected to reducing and denaturing SDS–PAGE. The biotin-fumagillin conjugate remains attached to the MetAPs only when bound covalently. As we have previously shown, biotin-fumagillin is bound covalently to human MetAP2 (shown here as a doublet due to proteolysis upon storage) (Fig. 2B, Lane 3). This covalent binding is competed by an excess amount of free TNP-470 (Fig. 2B, Lane 4). Like human MetAP2, MAP-2 is also bound to fumagillin covalently and as expected, its binding to MAP-2 is sensitive to competition by TNP-470 (Fig. 2B, Lanes 1 and 2). These observations indicate that MAP-2 is highly similar to human MetAP2 in its interaction with the fumagillin family of inhibitors.

3.3. *map-2 is required for the development of the* C. elegans *gonad*

As a first attempt to determine the role of *map-2* in *C. elegans*, we treated worms with ovalicin by including the drug in the growth media or injection (see Section 2). However, no phenotypic change was seen upon treatment with ovalicin. Since ovalicin contains such unstable functional groups as the epoxide that is critical for its activity, it is unclear whether the lack of effect of ovalicin reflects the absence of an in vivo role for methionine aminopeptidase activity in *C. elegans* or is due to the inability of an active drug to reach *map-2* expressing cells.

As an alternative approach to inhibiting *map-2* activity by ovalicin treatment, we examined the effect of interfering with *map-2* expression by RNAi. Of the 4 MetAP2 related *C. elegans* sequences, F53B6.5 and T27A8.3 are over 99% identical to each other at the base pair level, and are also 91% identical to *map-2* over a 350 bp region in the 3′ region of *map-2* (base pairs 845–1195). Given these high levels of similarity, dsRNA directed against the 3′ region of *map-2* could affect the transcript levels of all three genes [27,28]. Therefore, we determined if RNAi against the 5′ region of *map-2*, which shares no homology with F53B6.5 or T27A8.3, could effectively interfere with *map-2* expression. We injected dsRNA corresponding to full-length *map-2*, and the 5′ and 3′ regions independently (Fig. 3A and methods). The progeny of injected animals were lysed and subjected to Western blotting with an antibody raised against human MetAP2 that we found to cross-react with recombinant worm MAP-2 protein. In control lysates, this antibody recognizes a protein of approximately 50 kDa, which corresponds to the predicted size of MAP-2 (Fig. 3A, Lanes 1 and 5). By contrast, no protein was detected in any of the *map-2* RNAi treated animals (Fig. 3A, Lanes 2–4). Thus,

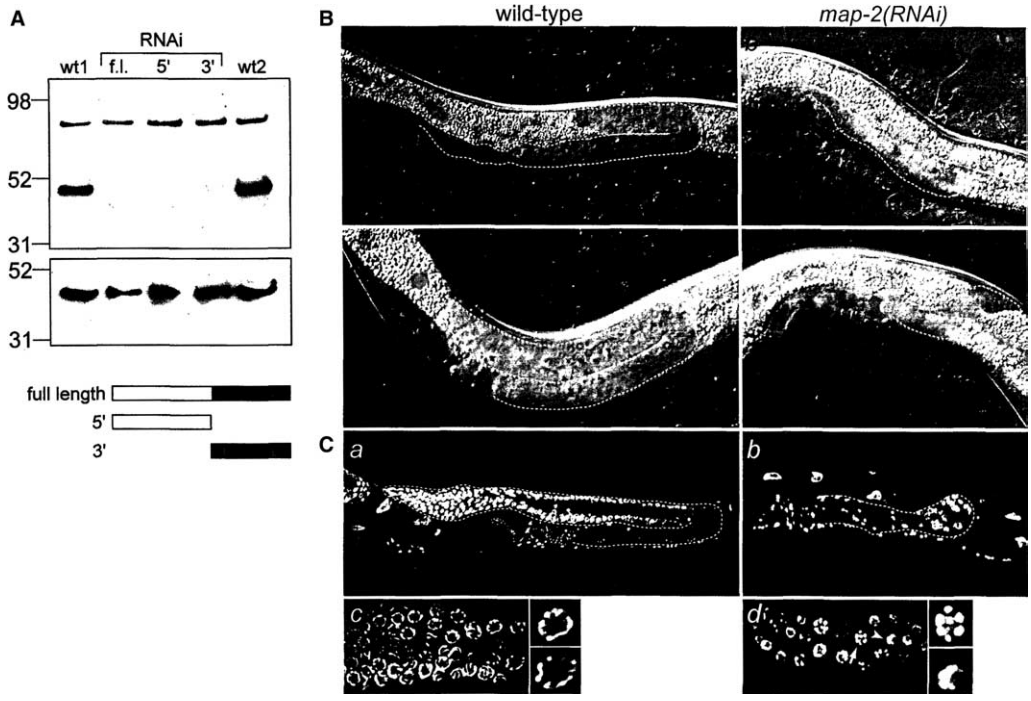

Fig. 3. *map-2* RNAi blocks germline development. (A) Western blot showing cross reactivity of an anti-METAP2 antibody with a protein of expected size in wild-type *C. elegans* lysates (Lanes 1 and 5) but not in protein lysates from *map-2(RNAi)* animals (Lanes 2–4). Lane 1: lysate from progeny of animals injected with TE buffer. Lanes 2–4: lysate from progeny of animals injected with dsRNA corresponding to the fragments of *map-2* shown below the blots. Lane 5: untreated wild-type N2 lysate. Bottom panel shows staining of the same samples with an anti-tubulin antibody as a loading control. Gray and black areas in drawing of *map-2* indicate regions of 45% and 91% identity with F53B6.5 and T27A8.3, respectively. (B) Nomarski DIC microscopy images of wild-type *C. elegans* (left panels) and *map-2(RNAi)* animals (right panels). *a* and *b* show late L3/early L4 animals (as judged by vulva development) and *c* and *d* show adult animals. (C) Propidium iodide DNA staining of wild type adult animals (*a*,*c*) and *map-2(RNAi)* adult animals (*b*,*d*). *a* and *b* are an overview of an entire gonad arm, while *c* and *d* show a higher magnification. Small panels show two typical pachytene nuclei from the wild-type gonad and examples of the discrete foci (arrow in *d*) or less condensed (arrowhead in *d*) nuclei observed in *map-2(RNAi)* animals.

all three *map-2* RNAi constructs efficiently interfere with *map-2* expression.

In addition to Western blot analysis, the progeny of injected wild-type animals was examined for mutant phenotypes. In all cases, embryos appeared to develop normally and hatched at similar times as wild-type control embryos. No delays in larval development were observed, and movement of RNAi animals was normal, indicating no obvious abnormalities in nervous system or muscle development. However, each of the three RNAi injections caused larvae to develop into sterile adults. Examination of the *map-2* sterile animals by Nomarski DIC microscopy showed that these animals have small gonad arms, with few, if any, germ cells present. Thus, *map-2* appears to be required for *C. elegans* gonad development.

As RNAi against the 5′ region of *map-2* interfered as efficiently with *map-2* expression as RNAi against full length or 3′ *map-2*, and all three RNAi constructs produced the same phenotype, the 5′ region was used in all further RNAi experiments.

3.4. Inactivation of map-2 causes a defect in germ-cell proliferation and differentiation

To examine the defects caused by *map-2* RNAi in more detail, the different larval stages of *map-2(RNAi)* animals were studied both by Nomarski DIC microscopy and by staining with the DNA intercalating dye propidium iodide (P.I.). All somatic tissues appeared to form normally, including cells of the uterus, gut, hypodermis and pharynx – which was actively pumping. In contrast, neither arm of the gonad developed to the wild type size. Although a small number of germ cells are formed, differentiation of sperm and oocytes was not observed (Fig. 3B, compare panels *a* and *c* with panels *b* and *d*). In addition, condensation of the DNA of the germ cells was abnormal. In wild type animals, germ cells are formed at the distal end of the gonad. Moving proximally, germ cells enter meiosis and arrest at pachytene of prophase of meiosis I until around the time they pass the U-shaped flexure in the gonad. At this point the chromosomes condense further as the germ cells enter diakinesis and oocytes are formed. In *map-2(RNAi)* animals, the typical threadlike appearance of the paired homologous chromosomes in pachytene (Fig. 3C, panel *c*) is not observed. Instead, some germ cells appear only partly condensed, while the DNA in others appears as a number of discrete foci (Fig. 3C, panel *d*). In the latter case, more than 6 foci are observed, indicating a possible defect in chromosome pairing. Thus, *map-2* appears to be essential for germ-cell proliferation and differentiation.

3.5. map-2 RNAi causes a cell-intrinsic defect in germ cell proliferation

The *C. elegans* adult reproductive system consists of two gonadal arms, each composed of 5 pairs of somatic sheath cells, filled with germ cells in various stages of development (reviewed in [29]). Each gonad arm is capped at its distal end

by a distal tip cell (DTC), which secretes a signal required for development of the germline. The lack of germ cell proliferation in *map-2(RNAi)* animals could be due to a cell intrinsic defect, or to a defect in these somatic gonadal tissues. To distinguish between these possibilities, we examined sheath cell formation in *map-2(RNAi)* animals and performed *map-2(RNAi)* in a mutant background in which somatic cells are not affected by RNAi.

To determine if gross abnormalities in the somatic gonad exist in *map-2(RNAi)* animals, we examined a GFP marker for development of the sheath cells. In wild-type animals during gonadogenesis and in adults, the *lim-7::GFP* reporter gene is expressed in the 4 most distal sheath cell pairs (Fig. 4A and C) [20]. Similarly, in *map-2* RNAi animals, we observed expression of *lim-7::GFP* at the distal end of the gonad arms (Fig. 4B and D). Thus, *map-2(RNAi)* animals express a marker for gonad development in the appropriate tissue at the correct stages of development.

To determine if *map-2* functions in a germ cell-intrinsic fashion, we examined the effect of inactivating *map-2* by RNAi in an *rrf-1* mutant background. The *rrf-1* gene encodes an RNA-directed RNA polymerase required for the amplification of the RNAi signal specifically in somatic tissues [21]. Thus, *rrf-1* mutant animals lack an RNAi response in the soma. If *map-2* function is restricted to the germline, *map-2* RNAi in *rrf-1* mutant animals would be expected to produce an identical phenotype to *map-2* RNAi in wild-type animals. We injected *map-2* dsRNA into *rrf-1(pk1417)* mutant animals and examined their progeny. As with *map-2* RNAi in wild-type animals, *map-2* RNAi in *rrf-1* mutants produced 100% sterile offspring. Both by Nomarski DIC microscopy of live animals and by PI staining of the DNA of fixed adults, the phenotype of the *rrf-1; map-2(RNAi)* animals was indistinguishable from that observed upon *map-2* RNAi in a wild-type background. This indicates that *map-2* does not play an essential role in somatic tissues.

Although RNAi by injection has been shown to phenocopy the effect of many strong loss-of-function alleles [27,28], it remains possible that certain developmental stages or tissues of *C. elegans* are refractory to *map-2* RNAi, and that lack of gonad development is not the full *map-2* null phenotype. However, the fact that *map-2* RNAi dramatically reduces MAP-2 protein expression argues against this possibility. Therefore, based upon our findings we conclude that *map-2* most likely acts in the germline and regulates germline development and/or proliferation in a cell-intrinsic fashion in *C. elegans*.

4. Discussion

In the present study, we examined the role of type 2 MetAPs in the development of *C. elegans* using RNA interference. We identified a predicted ORF, which we termed *map-2*, with a high degree of similarity with human and yeast MetAP2 over the entire length of the protein. Biochemical analysis demonstrates that MAP-2 protein possesses methionine aminopeptidase activity, and is sensitive to inhibition by the fumagillin analog TNP-470 like its human and yeast counterparts. Our analysis of the loss-of-function phenotype of the *map-2* gene indicates that *map-2* is required for germ-cell proliferation in a tissue-specific manner.

Although the biochemical function of type 2 MetAPs – the removal of amino-terminal methionines – appears to be a general one, inactivation of MetAP2 has been shown to cause tissue-specific defects in different organisms. For example, most mouse cells are sensitive to inhibition by TNP-470 [30]. By contrast, TNP-470 is highly selective toward human endothelial cells without significantly affecting other cell types [18,30,31]. In *Drosophila*, weak alleles of the MetAP2 ortholog, *DMAP2*, cause a roughened eye phenotype, with ommatidial rotation defects and a reduced size of the ventral half of the eye [32]. In addition, the L5 wing vein is often abnormally branched with extra vein material. Putative loss-of-function alleles are lethal, but analysis of mutant cell clones in the eye indicates an essential role for *DMAP2* in cell growth. Thus, in four different model systems, MetAP2 appears to act in a distinct set of tissues.

The different phenotypes observed in various model organisms in response to downregulation of MetAP2 level or activity

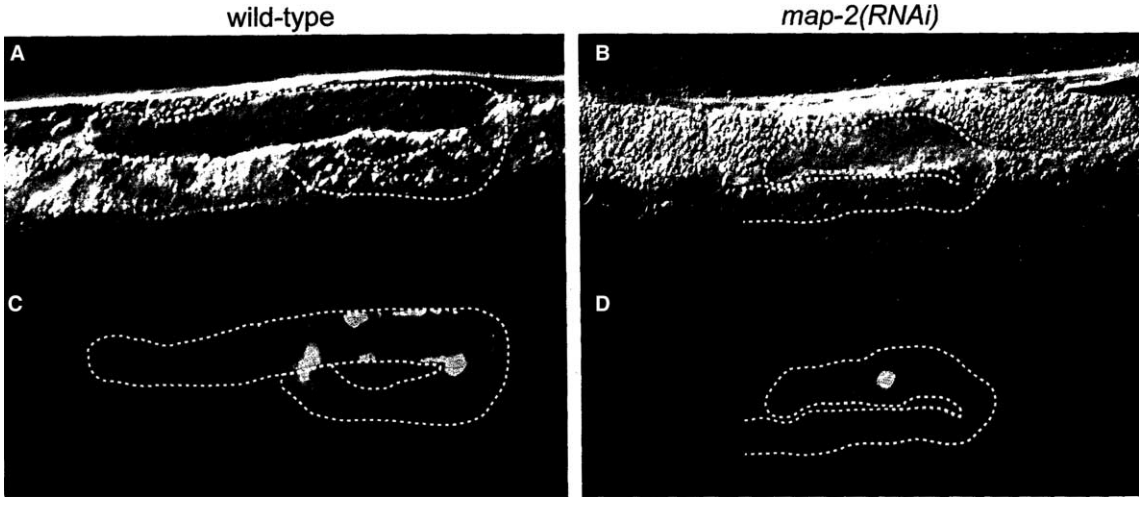

Fig. 4. *lim-7::GFP* is expressed in sheath cells of *map-2(RNAi)* animals. Nomarski DIC microscopy images (A, B) and corresponding fluorescence microscopy images (C, D) of a wild type adult animal (left panels) and a *map-2(RNAi)* adult animal (right panels).

suggest that different species and different cell types within the same species have diverged in their dependence on MetAP2. How might this divergence come about? A few possibilities exist. First, MetAP2 in higher eukaryotes may have distinct substrate specificity, and the particular protein substrates may vary between organisms. Given the general nature of methionine aminopeptidase activity and conservation in sequence, it appears unlikely that such specificity of MetAP2 has developed. A second possibility is that MetAP2 targets a large similar set of proteins in each organism and the difference in dependence on MetAP2 reflects a difference in dependence upon the homologous MetAP2 substrates. Finally, it is possible that the critical MetAP2 targets are the same in each organism, but the biological processes or pathways in which these proteins function differ in each organism.

In addition to their function as methionine aminopeptidases, eukaryotic MetAP2 proteins have evolved to regulate protein synthesis by preventing the phosphorylation and inactivation of the α-subunit of eukaryotic initiation factor-2 (eIF2) [33,34]. This function appears to be mediated by a lysine rich domain and a glycosylation site in an N-terminal extension of the protein that is specific to eukaryotic MetAP2 [35,36]. Although *C. elegans* MAP-2 shares the N-terminal extension with other eukaryotic MetAP2 enzymes, the lysine rich domain and the glycosylation site are poorly conserved. It is unclear therefore whether MAP-2 has a function in regulating eIF2.

Acknowledgements: We are grateful to Sander van den Heuvel and Marc Vidal for their generous support during different phases of this work and to Dr. Yie-Hwa Chang for the anti-human MetAP2 antibody. We thank David Greenstein for the *lim-7::GFP* reporters strain and Tim Schedl for the *glp-1* gain-of-function mutant strain. We also thank Geraldine Seydoux for critical comments on the manuscript. Research support was provided in part by an NIH grant (CA078743) to J.O.L. M.B. was supported by a Boehringer Ingelheim Fonds PhD grant and a Leukemia Research Foundation postdoctoral fellowship.

References

[1] Bradshaw, R.A., Brickey, W.W. and Walker, K.W. (1998) Trends Biochem. Sci. 23, 263–267.
[2] Lowther, W.T., Matthews, B.W., Bradshaw, R.A. and Yi, E. (2002) Chem. Rev. 102, 4581–4608.
[3] Miller, C.G., Kukral, A.M., Miller, J.L. and Movva, N.R. (1989) J. Bacteriol. 171, 5215–5217.
[4] Chang, S.Y., McGary, E.C. and Chang, S. (1989) J. Bacteriol. 171, 4071–4072.
[5] Arfin, S.M., Kendall, R.L., Hall, L., Weaver, L.H., Stewart, A.E., Matthews, B.W. and Bradshaw, R.A. (1995) Proc. Natl. Acad. Sci. USA 92, 7714–7718.
[6] Li, X. and Chang, Y.H. (1995) Proc. Natl. Acad. Sci. USA 92, 12357–12361.
[7] Dummitt, B., Fei, Y. and Chang, Y.H. (2002) Protein Pept. Lett. 9, 295–303.
[8] Serero, A., Giglione, C., Sardini, A., Martinez-Sanz, J. and Meinnel, T. (2003) J. Biol. Chem. 278, 52953–52963.
[9] Ingber, D., Fujita, T., Kishimoto, S., Sudo, K., Kanamaru, T., Brem, H. and Folkman, J. (1990) Nature 348, 555–557.
[10] Lowther, W.T., McMillen, D.A., Orville, A.M. and Matthews, B.W. (1998) Proc. Natl. Acad. Sci. USA 95, 12153–12157.
[11] Liu, S., Widom, J., Kemp, C.W., Crews, C.M. and Clardy, J. (1998) Science 282, 1324–1327.
[12] Griffith, E.C., Su, Z., Niwayama, S., Ramsay, C.A., Chang, Y.H. and Liu, J.O. (1998) Proc. Natl. Acad. Sci. USA 95, 15183–15188.
[13] Turk, B.E., Su, Z. and Liu, J.O. (1998) Bioorg. Med. Chem. 6, 1163–1169.
[14] Klein, C.D. and Folkers, G. (2003) Oncol. Res. 13, 513–520.
[15] Sin, N., Meng, L., Wang, M.Q., Wen, J.J., Bornmann, W.G. and Crews, C.M. (1997) Proc. Natl. Acad. Sci. USA 94, 6099–6103.
[16] Griffith, E.C., Su, Z., Turk, B.E., Chen, S., Chang, Y.H., Wu, Z., Biemann, K. and Liu, J.O. (1997) Chem. Biol. 4, 461–471.
[17] Kusaka, M., Sudo, K., Matsutani, E., Kozai, Y., Marui, S., Fujita, T., Ingber, D. and Folkman, J. (1994) Br. J. Cancer 69, 212–216.
[18] Yanase, T., Tamura, M., Fujita, K., Kodama, S. and Tanaka, K. (1993) Cancer Res. 53, 2566–2570.
[19] Wood, W., and the community of *C. elegans* researchers (1988) Cold Spring Harbor Laboratory Press, Cold Spring Harbor, NY.
[20] Hall, D.H., Winfrey, V.P., Blaeuer, G., Hoffman, L.H., Furuta, T., Rose, K.L., Hobert, O. and Greenstein, D. (1999) Dev. Biol. 212, 101–123.
[21] Sijen, T., Fleenor, J., Simmer, F., Thijssen, K.L., Parrish, S., Timmons, L., Plasterk, R.H. and Fire, A. (2001) Cell 107, 465–476.
[22] Reboul, J. et al. (2003) Nat. Genet. 34, 35–41.
[23] Timmons, L., Court, D.L. and Fire, A. (2001) Gene 263, 103–112.
[24] Boxem, M., Srinivasan, D.G. and van den Heuvel, S. (1999) Development 126, 2227–2239.
[25] Harlow, E. and Lane, D. (1999) Cold Spring Harbor Laboratory Press, Cold Spring Harbor.
[26] Ben-Bassat, A., Bauer, K., Chang, S.-K., Myambo, K., Boosman, A. and Chang, S. (1987) J. Bacteriol. 169, 751–757.
[27] Fire, A., Xu, S., Montgomery, M.K., Kostas, S.A., Driver, S.E. and Mello, C.C. (1998) Nature 391, 806–811.
[28] Tabara, H., Grishok, A. and Mello, C.C. (1998) Science 282, 430–431.
[29] Schedl, T. (1997) in: *C. elegans* II (Riddle, D.L., Blumenthal, T., Meyer, B.J. and Priess, J.R., Eds.), pp. 241–270, Cold Spring Harbor Laboratory Press, Plainview, NY.
[30] Wang, J., Lou, P. and Henkin, J. (2000) J. Cell. Biochem. 77, 465–473.
[31] Yamamoto, T., Sudo, K. and Fujita, T. (1994) Anticancer Res. 14, 1–3.
[32] Cutforth, T. and Gaul, U. (1999) Mech. Dev. 82, 23–28.
[33] Datta, B., Chakrabarti, D., Roy, A.L. and Gupta, N.K. (1988) Proc. Natl. Acad. Sci. USA 85, 3324–3328.
[34] Datta, B., Ray, M.K., Chakrabarti, D., Wylie, D.E. and Gupta, N.K. (1989) J. Biol. Chem. 264, 20620–20624.
[35] Datta, R., Choudhury, P., Bhattacharya, M., Soto Leon, F., Zhou, Y. and Datta, B. (2001) Biochimie 83, 919–931.
[36] Datta, R., Choudhury, P., Ghosh, A. and Datta, B. (2003) Biochemistry 42, 5453–5460.